Current Optics and Photonics
Vol. 3, No. 6, December 2019, pp. 496-501

ISSN: 2508-7266(Print) / ISSN: 2508-7274(Online)
DOI: https://doi.org/10.3807/COPP.2019.3.6.496

Transmission Matrix Noise Elimination for an Optical Disordered Medium

Lin Wang[1], Yangyan Li[1], Yu Xin[1]*, Jue Wang[2], and Yanru Chen[1]

[1]*School of Electronic and Optical Engineering, Nanjing University of Science and Technology, Nanjing 210094, China*
[2]*College of Electrical, Energy and Power Engineering, Yangzhou University, Yangzhou 225127, China*

(Received August 20, 2019 : revised October 7, 2019 : accepted October 18, 2019)

We propose a method to eliminate the noise of a disordered medium optical transmission matrix. Gaussian noise exists whenever light passes through the medium, during the measurement of the transmission matrix and thus cannot be ignored. Experiments and comparison of noise eliminating before and after are performed to illustrate the effectiveness and advance presented by our method. After noise elimination, the results of focusing and imaging are better than the effect before noise elimination, and the measurement of the transmission matrix is more consistent with the theoretical analysis as well.

Keywords : Disordered medium, Transmission matrix, Noise eliminating, Hadamard basis
OCIS codes : (290.5820) Scattering measurements; (030.4280) Noise in imaging systems; (090.2880) Holographic interferometry; (050.5080) Phase shift

I. INTRODUCTION

Research on light passing through disordered scattering medium has experienced an obvious burst of interest over the last decade. Unlike a wavefront propagating in a uniform medium or free space, light spreads unexpectedly in a disordered medium such as biological tissues, white powders and random nanostructures. Disordered scattered particles arranged in the medium will hinder the free transmission of the optical wave and cause the direction of wave vector to change randomly. This phenomenon will bring completely scrambled distributions in both transmitted and back scattering directions, bearing no clear relation to the incident waveform [1-3].

Nonetheless, recent studies have shown that the speckle patterns can be controlled under conditions where the wavefront can be acquired and the disordered medium is stationary during the wavefront recording process [4-6]. Vellekoop *et al*. has demonstrated that wave focusing [7, 8] and Choi *et al*. proved spatial resolution in imaging can be enhanced by the use of a disordered medium beyond the limits of a conventional imaging system [9, 10]. In essence, these methods use the linearity and time-reversal symmetry of the wave propagation, a 'transmission matrix' (**TM**) describes the input-output response of a disordered medium, which not only connects the incident waves with the speckle patterns but also provides penetrating insights on the disordered medium. In these applications such as pattern reconstruction and optical focusing, which depend on the **TM**, the accuracy of measurement plays the most important role for bringing the direct effects to the results.

Following these pioneering works, researchers pointed out that varieties of factors will affect the measurement accuracy of the **TM**, such as the characteristics of polarization, the choice of reference and the modulation of the incident wave [11-13] and the noise level [14]. In this paper, we report a principle to eliminate some adverse impacts in the measurement process. A new equation describing the **TM** with contributions of Gaussian noise is proposed closer to the actual situation which can help us to remove the noise.

II. METHODS

In previous works, researchers have considered that, light

*Corresponding author: yxin@njust.edu.cn, ORCID 0000-0001-8788-8679
Color versions of one or more of the figures in this paper are available online.

transport through a scattering medium can be characterized by a **TM** model: $E_m^{\text{out}} = \sum_n t_{m,n} E_n^{\text{in}}$, the complex coefficients $t_{m,n}$ connecting the nth input free mode or channel and the mth output free mode, is an entity of the **TM**, the model describes itself as Eq. (1):

$$\mathbf{E}^{\text{out}} = \begin{bmatrix} E_1^{\text{out}} \\ E_2^{\text{out}} \\ \vdots \\ \vdots \\ E_m^{\text{out}} \end{bmatrix} = \begin{bmatrix} t_{1,1} & t_{1,2} & \cdots & t_{1,n} \\ t_{2,1} & \ddots & & \\ \vdots & & \ddots & \\ \vdots & & & \ddots \\ t_{m,1} & & & t_{m,n} \end{bmatrix} \begin{bmatrix} E_1^{\text{in}} \\ E_2^{\text{in}} \\ \vdots \\ \vdots \\ E_n^{\text{in}} \end{bmatrix} = \mathbf{T}\mathbf{E}^{\text{in}}. \quad (1)$$

The transmission matrix **T** stands for the optical transformation of the disordered medium, the incident optical field $\mathbf{E}^{\text{in}}$ is reorganized into an $n \times 1$ vector and the relative output field $\mathbf{E}^{\text{out}}$ is described by an $m \times 1$ vector as well. In this model, the entries (or elements) of **T** are assumed to obey the complex Circular Gaussian distribution with zero mean and variance $\sigma^2 = 1$ in both real and imaginary parts.

The model in Eq. (1) is simple enough and helpful for us to obtain the optical quantification effect of the disordered medium. Nevertheless, we believe that the factor of noise makes its contributions to the output optical field in practical applications, using the model in Eq. (1) ignores the effect of noise, which shall prevent us from knowing the true nature of the transmission matrix, that is the disordered medium. Thus, we propose an improved model of **TM** calculating the noise as Eq. (2):

$$\mathbf{E}^{\text{out}} = \mathbf{T}\mathbf{E}^{\text{in}} + \mathbf{N}, \quad (2)$$

where **N** denotes the 1-dimensional noise matrix, specifically, in Eq. (2) and in Eq. (3), the **N** is an $m \times 1$ vector as well. For any stationary disordered medium, the noise matrix is determined by the system and is static.

To eliminate the effect of noise, we should first measure all the responses of the system's basis input free modes, as well as the known the unitary matrix. The optimal and most efficient unitary matrix has been proved to be the Hadamard matrix, in which the elements are either +1 or -1 in phase, and any two rows (or two columns) are orthogonal as the input basis. Implementing the positive and negative Hadamard matrix sequentially as Eq. (3) shows:

$$\begin{cases} \mathbf{E}_{\text{pos}}^{\text{out}} = \mathbf{T}\mathbf{H}_n + \mathbf{N} \\ \mathbf{E}_{\text{neg}}^{\text{out}} = \mathbf{T}(-1 \times \mathbf{H}_n) + \mathbf{N} \end{cases}. \quad (3)$$

The transmission matrix can be solved by:

$$\mathbf{T} = (\mathbf{E}_{\text{pos}}^{\text{out}} - \mathbf{E}_{\text{neg}}^{\text{out}})\mathbf{H}_n^{\text{T}} \times 0.5n^{-2}, \quad (4)$$

where $\mathbf{E}_{\text{pos}}^{\text{out}}$ and $\mathbf{E}_{\text{neg}}^{\text{out}}$ are the complex field of responses taking positive Hadamard matrix and negative Hadamard matrix as the system's input waves, respectively. $\mathbf{H}_n$ is a Hadamard matrix with dimension of $n \times n$, the number n is restricted by ($n = 2^i$, $i = 1, 2, 3...$), in which the elements are either +1 or -1 in phase, and any two rows (or two columns) are orthogonal as the input basis [15-18]. The mark $(\cdot)^{\text{T}}$ represents the complex matrices' conjugate transpose operation.

III. EXPERIMENTS AND RESULTS

The experimental setup is shown in Fig. 1. A cw laser beam ($\lambda = 532$ nm) passes through the first microscope (NA = 0.25) and a Fourier lens ($f = 100$ mm) which are combined for alignment and expansion. A pinhole is placed on the focal plane of the microscope, working as a spatial filter. The collimated beam reflected by BS1 is reflected by BS2 again to illuminate the phase-only spatial light modulator (SLM, Holoeye PLUTO-VIS-016). The screen of SLM modulates the phase of the plane wave light into the incident wave front. The other objective (NA = 0.75) acts as a beam concentrator to the disordered medium sample. In our setup, the medium is produced by Zinc Oxide (ZnO) particles of 50 nm in diameter, with 70 um thick and 7.2 ± 3 um mean free path. The transmitted light is collected by the last microscope with NA = 0.75. The speckle-like output is recorded by the charge-coupled device

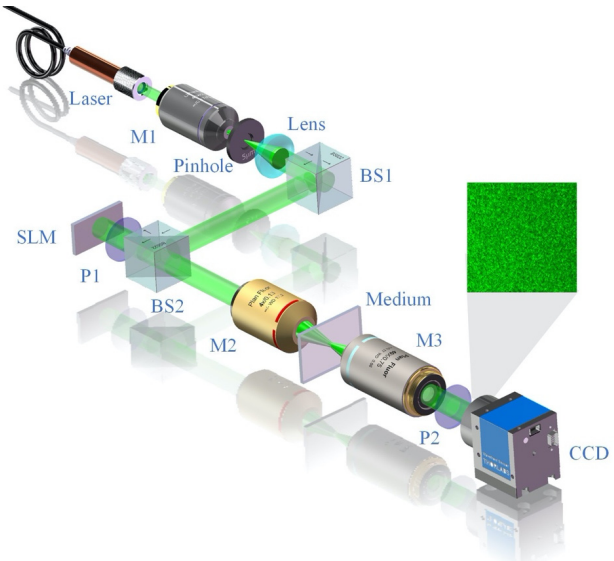

FIG. 1. Experimental setup, measuring the transmission matrix. M1, M2, M3: microscope 1, 2 and 3; BS: beam splitter; P1, P2: polarizer 1 and 2, their long axis are adjusted in horizontal both. The M2 and M3 are placed in coupling position with each other, but the SLM and CCD are not specifically required to be placed on the backfocal plane of M2 and M3, respectively, because every element between SLM and CCD consists the transmission system.

(CCD, Thorlabs, DCU224C, 1280*1024, with 4.64×4.65 um^2 pixel size) placed behind of polarizer 2. Two polarizers P1 and P2 are placed in front of the SLM and the CCD, respectively, to make sure the input-output relationship is limited in scalar, especially to make sure the SLM works as phase-only modulator along with incident light polarized in the horizontal direction.

In our experiment, the scattering sample is composed of zinc oxide (ZnO) particles with diameter of 50 nm, sprayed onto a microscope cover glass, with 70 um thick and 7.2 ± 3 um mean free path, with these characteristics, the average transmission of our strongly disordered sample is $T \approx 0.1\%$.

In order to obtain the coefficients t_{mn}, the output field must be recorded as complex distribution as well, a technique called phase-shifting interferometry is applied to resolve the complex amplitude of output [19-21]. The mth output field can be calculated from $E_m^{out} = (I_m^1 + I_m^5 - 2I_m^3) + 2 * j(I_m^2 - I_m^4)$, where I_m^1 to I_m^5 are the CCD captured intensities at shift amount of 0, $\pi/2$, π, $3\pi/2$, 2π, respectively.

Considering the entrance pupil of objective (NA = 0.75), limited pixels of SLM are active or detectable and form a circular area, this area contains two main sections of a rectangular controlled part which inscribes the pupil and a reference part which occupies the remaining pixels. These two parts make the system an on-axis interferometer. After loading rows (or columns) of the Hadamard matrix to the SLM screen and saving corresponding pictures of five-step shifts captured by the CCD, we can calculate out the transmission matrix. In our experiment, 32×32 incident modes are employed, taking 640×640 SLM pixels, and the number of pixels employed from the CCD is 256×256. The measurement process requires approximately 15 minutes, fixed modulator refresh rate is the main reason for time consumption. Decreasing the pixels of SLM and CCD used will accelerate the process procedure but the accuracy will be reduced simultaneously. After performing all the Hadamard basis to complete the measurement, the property of **TM** can be expressed as:

$$\begin{cases} \mathbf{E}^{out} = \mathbf{T}\mathbf{E}^{in} + \mathbf{N} \\ \mathbf{T}^{T}(\mathbf{E}^{out} - \mathbf{N}) = \mathbf{E}^{in} \end{cases} \tag{5}$$

Figure 2 shows two simple applications exploiting the **TM** of a disordered medium based on Eq. (5) and phase conjugation [22-27]. a pattern like the letter N is displayed and illuminated in the SLM. Then modulated light goes through and gets scattered by the disordered medium. The speckle captured by the CCD is regarded as the pattern multiplied by the **TM**. By using Eq. (5) the input pattern can be reconstructed. In other words, the letter N in this example will show up. The second row of Fig. 2 shows a more practical application of optical focusing or imaging. Designed focusing or imaging effects are generated in the computer firstly. Then multiplying it by the transpose

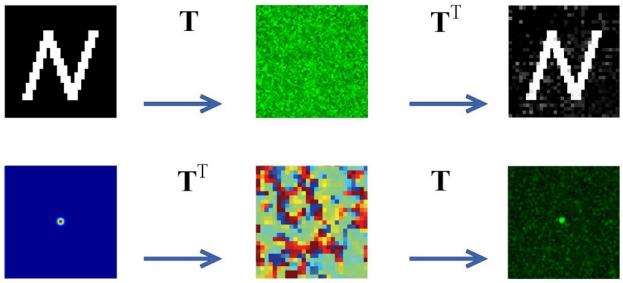

FIG. 2. Two simple applications. The first row shows the process of digital reconstruction, we display one binary pattern of letter N on the SLM and capture the relative speckle image on CCD plane, then reconstruct the pattern digitally from this speckle image. The second row shows the optical focusing or imaging. The first subfigure in this row is the target we want, transform this target by $\mathbf{T}^T$, we thus have the pattern (in phase map, $[0, 2\pi]$), as the second subfigure shows, then display this pattern on SLM, the focusing point is immediately produced on the CCD plane.

conjugation of **TM** gives us the relative phase pattern that looks like the middle picture in the second row, displaying the pattern onto the SLM (in gray scale), the desired focusing points or images will appear in the camera rapidly.

The best way to verify the physical relevance between our measured **TM** and the optical system is to perform an optical focusing or imaging process on arbitrary output locations. That is to say, to apply the second application shown in Fig. 2. When we calculate the modulation phase pattern from a target we want, by using Eq. (5), and put the phase pattern on the SLM screen, a focus or image shape will appear on the CCD.

The most significant advantage of our method is the promotion of signal to noise ratio (SNR). Because the intensity of transmitted light over a disordered medium is very weak, the desired signal we modulated is easily drowned in the noise background. Figure 3 shows the comparison of these two situations at the same focus position. In Fig. 3(b) it is clear that the contrast of the focus is obviously improved. Figure 3(c) shows the SNR has been enhanced about 8 dB = $10\log(225/100)$. The raw SNR of a light passing through the disordered medium is indicated by the transmittance of the scattering sample and the number of controlled incident modes, in our experiment, the transmittance is $T \approx 0.1\%$ and with 32×32 incident modes.

Besides, we tried simple image experiments. In principle, the process of imaging is equivalent to controlling neighboring pixels focus, but needs more energy to be controllable and thus requires a high SNR. Figure 4 shows the vertical and horizontal lines as simple images and an initial letter of NJUST in Fig. 4(c).

In order to get a high SNR focusing or imaging results, fundamentally, increasing the number of modes of the incident wave is the most straightforward idea. While the

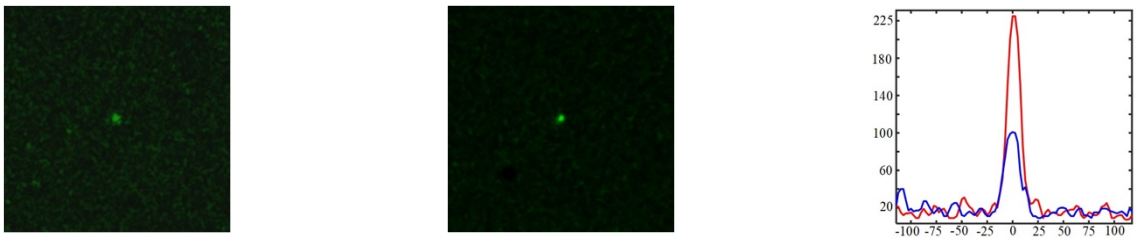

(a) (b) (c)

FIG. 3. The comparison of single point focus of two situations. (a) and (b) show the single focus on the CCD plane before and after noise elimination. The blue line and red line in (c) indicate the plot of the peaks in (a), (b), respectively.

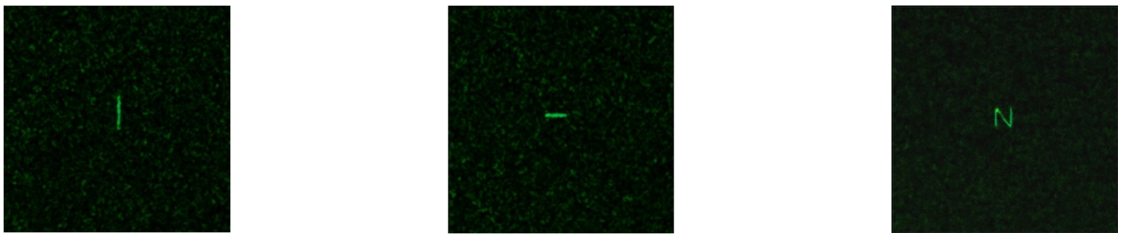

(a) (b) (c)

FIG. 4. Simple image. (a) (b) vertical and horizontal lines imaged at the CCD, (c) the N letter imaged at the CCD plane.

proportion of the modulation part increases, more controllable modes are in use, as un-modulated portions will have an adverse effect on the result. However, increasing the modes of the incident wave will make the burden increase significantly not only in data acquirement, but also in data processing. Time cost increased to about one hour when 64×64 input modes participated according to our experience, and a much larger dimension of data is very difficult and nearly cannot be calculated. With these difficulties, our method to improve on the accuracy of the **TM**'s measurement, provides an easy and cost-effective choice to get satisfactory results.

IV. DISCUSSION

The transmission matrix singular values (or eigenvalues) guarantee the maximal and minimal transmitted fluxes. The corresponding eigenvectors are the optimal input wavefronts that the SLM should modulate. To study the eigenvalues, we perform the SVD tool:

$$\mathbf{T} = \mathbf{U}\Sigma\mathbf{V}^{\mathrm{T}}, \tag{6}$$

where Σ is a diagonal matrix with non-negative real numbers on the diagonal, also called eigenvalues or singular values. The **V** and **U** are unitary matrices mapping the input channels ($\mathbf{E}^{\mathrm{in}}$) to eigenchannels, and eigenchannels to output channels ($\mathbf{E}^{\mathrm{out}}$), respectively.

In our paper, the measured **TM** with $m \times n$ ($m > n$) dimension meets the independent Gaussian distribution, thus the distribution of eigenvalues of $\mathbf{T}\mathbf{T}^{\mathrm{T}}/m$, asymptotically approaches the Marčenko-Pastur (M-P) law [28, 29], when $c = m/n$ it reads:

$$\rho(\tau) = \frac{1}{2c\pi\tau}\sqrt{(a-\tau)(\tau-b)}, \tag{7}$$

where τ are the entries of Σ decomposed by the SVD in Eq. (6), $\tau_{\min} = b = (1-\sqrt{c})^2$ and $\tau_{\max} = a = (1+\sqrt{c})^2$. In order to simplify the calculation and without loss of generality, we take the number of $m = n = 1024$, that is to say we can select a sub-area with dimension of 32×32 from $\mathbf{E}^{\mathrm{out}}$. Thus in Figs. 5 and 6, $c = 1$ and the RMT's prediction is $0 \le \tau \le 4$. We use the Empirical Distribution Functions (EDF) to describe the distribution of singular values because our **TM**'s dimension is limited while the Random Matrix is theoretically infinite. Figures 5(a) and 5(b) show the Empirical Distribution Functions (EDF) of singular values of **TM** based on measurement results of Eqs. (1) and (4), respectively. In this figure, the horizontal axis is the range of singular values, and the vertical axis is the relative probability density. Obviously, the distribution of noise elimination is more proper than the non-eliminating one, the singular values in Fig. 5(b) which beyond the range is less than the singular values in Fig. 5(a).

However, as the laser beam is a coherent source, which causes significant correlation effects between neighboring or contiguous pixels on the CCD [30]. From Fig. 5, it is obvious that, most yellow bins don't reach the blue lines, it means the interference does weaken the transmitted fluxes. To avoid this, we pick the 1024 pixels from a 256×256

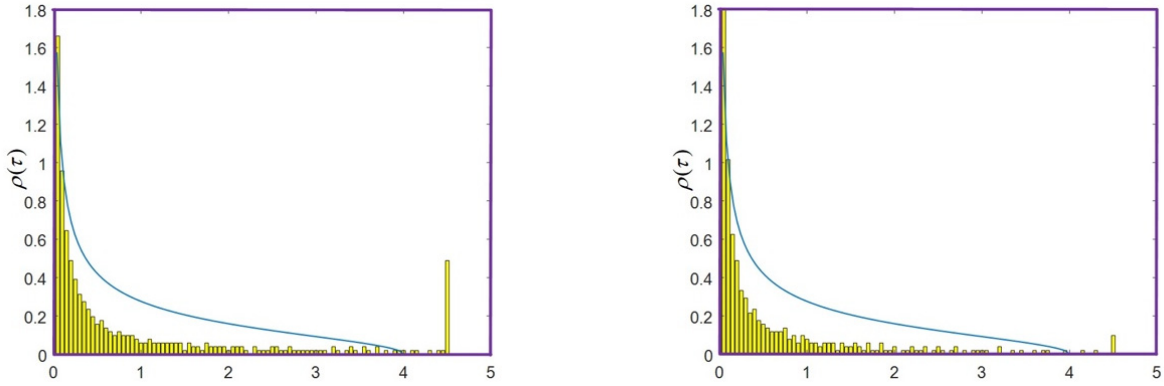

FIG. 5. The EDF of singular values of $\mathbf{TT}^{\mathrm{T}} / m$, c= 1. Yellow bins in (a), (b) plot the histogram of the $m = n$ = 1024 eigenvalues of $\mathbf{TT}^{\mathrm{T}} / m$ before and after noise eliminating, respectively. Blue lines in each figure are the prediction as M-P law model, x axis is the normalized singular value τ. The most right-side bins in (a) exceeds the maximum value of M-P law indicated.

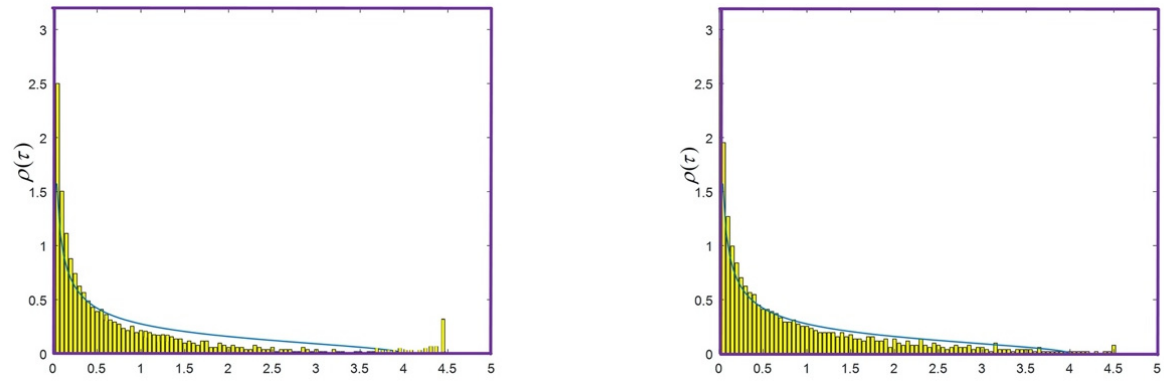

FIG. 6. The EDF of singular values of $\mathbf{TT}^{\mathrm{T}} / m$, c= 1, without correlation effect. Yellow bins in (a), (b) plot the histogram of the $m = n$ = 1024 eigenvalues of $\mathbf{TT}^{\mathrm{T}} / m$ before and after noise eliminating, respectively. Blue lines in each figure are the prediction as M-P law indicated.

output mode randomly, instead of the continuous pixels above.

The existence of correlations prevents the generation of truly independent random numbers through coherent diffusion. Figure 6 shows the results with and without noise elimination, unlike in Fig. 5, the transmission eigenvalues calculated in Fig. 6 have been de-correlated. After the de-correlation, the output modes are closer to the random distribution, which means the optical transform of the disordered medium is a naturally random process.

V. CONCLUSION

In summary, our proposed method updates the model both in **TM** measurement and calculating. We first developed an equation connecting input and output free modes considering a noise factor which demonstrates the derivation of noise elimination progress. Then we experimentally performed the optical measurement of disordered medium's **TM**, achieving a series of results which are more consistent with theory. This method can significantly improve the accuracy of the **TM**'s measurement, improve the SNR of focusing passing though the scattering medium, and even more it will help us to approach the true nature of the optical disordered medium. This method is validated on three criteria: quality of pattern reconstruction, quality of focusing and distribution of singular values.

ACKNOWLEDGMENT

The research was supported by the National Nature Science Foundation of China (61675098, 61107011); We thank Xiuying Zhang in Institute of Advanced Materials (IAM), Nanjing University of Technology, for her greatest help in experimental sample preparation and characterization.

REFERENCES

1. A. Ishimaru, *Wave propagation and scattering in random media* (Academic Press, New York, USA, 1978), Vol. 2.
2. M. Kerker, *The scattering of light and other electromagnetic radiation: physical chemistry: a series of monographs* (Academic Press, New York, USA, 2013), Vol. 16, pp. 189-254.
3. P. W. Anderson, "Absence of diffusion in certain random lattices," Phys. Rev. **109**, 1492 (1958).
4. M. Cui and C. Yang, "Implementation of a digital optical phase conjugation system and its application to study the robustness of turbidity suppression by phase conjugation," Opt. Express **18**, 3444-3455 (2010).
5. S. M. Popoff, G. Lerosey, R. Carminati, M. Fink, A. C. Boccara, and S. Gigan, "Measuring the transmission matrix in optics: an approach to the study and control of light propagation in disordered media," Phys. Rev. Lett. **104**, 100601 (2010).
6. M. Kim, Y. Choi, C. Yoon, W. Choi, J. Kim, Q.-H. Park, and W. Choi, "Maximal energy transport through disordered media with the implementation of transmission eigenchannels," Nat. Photonics **6**, 581-585 (2012).
7. I. M. Vellekoop and A. P. Mosk, "Focusing coherent light through opaque strongly scattering media," Opt. Lett. **32**, 2309-2311 (2007).
8. A. P. Mosk, A. Lagendijk, G. Lerosey, and M. Fink, "Controlling waves in space and time for imaging and focusing in complex media," Nat. Photonics **6**, 283-292 (2012).
9. H. Cao, J. Y. Xu, D. Z. Zhang, S.-H. Chang, S. T. Ho, E. W. Seelig, X. Liu, and R. P. H. Chang, "Spatial confinement of laser light in active random media," Phys. Rev. Lett. **84**, 5584 (2000).
10. Y. Choi, T. D. Yang, C. Fang-Yen, P. Kang, K. J. Lee, R. R. Dasari, M. S. Feld, and W. Choi, "Overcoming the diffraction limit using multiple light scattering in a highly disordered medium," Phys. Rev. Lett. **107**, 023902 (2011).
11. Y. Guan, O. Katz, E. Small, J. Zhou, and Y. Silberberg, "Polarization control of multiply scattered light through random media by wavefront shaping," Opt. Lett. **37**, 4663-4665 (2012).
12. A. Drémeau, A. Liutkus, D. Martina, O. Katz, C. Schülke, F. Krzakala, S. Gigan, and L. Daudet, "Reference-less measurement of the transmission matrix of a highly scattering material using a DMD and phase retrieval techniques," Opt. Express **23**, 11898-11911 (2015).
13. X. Tao, D. Bodington, M. Reinig, and J. Kubby, "High-speed scanning interferometric focusing by fast measurement of binary transmission matrix for channel demixing," Opt. Express **23**, 14168-14187 (2015).
14. A. A. Farid and S. Hranilovic, "Capacity bounds for wireless optical intensity channels with gaussian noise," IEEE Trans. Inf. Theory **56**, 6066-6077 (2010).
15. J. Brenner and L. Cummings, "The hadamard maximum determinant problem," Am. Math. Mon. **79**, 626-630 (1972).
16. W. K. Pratt, J. Kane, and H. C. Andrews, "Hadamard transform image coding," Proc. IEEE **57**, 58-68 (1969).
17. J. A. Tropp, "Improved analysis of the subsampled randomized hadamard transform," Adv. Adapt. Data Anal. **3**, 115-126 (2011).
18. N. J. A. Sloane and M. Harwit, "Masks for hadamard transform optics, and weighing designs," Appl. Opt. **15**, 107-114 (1976).
19. J. Schwider, O. R. Falkenstoerfer, H. Schreiber, A. Zoeller, and N. Streibl, "New compensating four-phase algorithm for phase-shift interferometry," Opt. Eng. **32**, 1883-1886 (1993).
20. P. Hariharan, B. F. Oreb, and T. Eiju, "Digital phase-shifting interferometry: a simple error-compensating phase calculation algorithm," Appl. Opt. **26**, 2504-2506 (1987).
21. P. Hariharan, "Phase-shifting interferometry: minimization of systematic errors," Opt. Eng. **39**, 967-969 (2000).
22. M. Jang, H. Ruan, I. M. Vellekoop, B. Judkewitz, E. Chung, and C. Yang, "Relation between speckle decorrelation and optical phase conjugation (OPC)-based turbidity suppression through dynamic scattering media: a study on *in vivo* mouse skin," Biomed. Opt. Express **6**, 72-85 (2015).
23. D. Wang, E. H. Zhou, J. Brake, H. Ruan, M. Jang, and C. Yang, "Focusing through dynamic tissue with millisecond digital optical phase conjugation," Optica **2**, 728-735 (2015).
24. J. Park, C. Park, K. Lee, Y.-H. Cho, and Y. Park, "Time-reversing a monochromatic subwavelength optical focus by optical phase conjugation of multiply-scattered light," Sci. Rep. **7**, 41384 (2017).
25. Y. Shen, Y. Liu, C. Ma, and L. V. Wang, "Focusing light through scattering media by full-polarization digital optical phase conjugation," Opt. Lett. **41**, 1130-1133 (2016).
26. V. Bacot, M. Labousse, A. Eddi, M. Fink, and E. Fort, "Time reversal and holography with spacetime transformations," Nat. Phys. **12**, 972-977 (2016).
27. A. E. Fouda and F. L. Teixeira, "Statistical stability of ultrawideband time-reversal imaging in random media," IEEE Trans. Geosci. Remote Sens. **52**, 870-879 (2014).
28. A. Edelman and N. R. Rao, "Random matrix theory," Acta Numerica. **14**, 233-297 (2005).
29. V. A. Marčenko and L. A. Pastur, "Distribution of eigenvalues for some sets of random matrices," Math. USSR-Sbornik **1**, 457 (1967).
30. C. W. Hsu, S. F. Liew, A. Goetschy, H. Cao, and A. D. Stone, "Correlation-enhanced control of wave focusing in disordered media," Nat. Phys. **13**, 497-502 (2017).